J Multidisciplinary Scientific Journal

MDPI

Review

Hydrogen Production by Fluidized Bed Reactors: A Quantitative Perspective Using the Supervised Machine Learning Approach

Zheng Lian [1], Yixiao Wang [1], Xiyue Zhang [1], Abubakar Yusuf [1], Lord Famiyeh [1], David Murindababisha [1], Huan Jin [2,*], Yiyang Liu [3], Jun He [1,*], Yunshan Wang [4], Gang Yang [4] and Yong Sun [1,5,*]

1 Key Laboratory of Carbonaceous Wastes Processing and Process Intensification of Zhejiang Province, University of Nottingham Ningbo, Ningbo 315100, China; lianzhengsmart@gmail.com (Z.L.); shyyw12@nottingham.edu.cn (Y.W.); ssyxz4@nottingham.edu.cn (X.Z.); aiymashi@gmail.com (A.Y.); Lord.Famiyeh@nottingham.edu.cn (L.F.); DAVID.MURINDABABISHA@nottingham.edu.cn (D.M.)
2 School of Computer Science, University of Nottingham Ningbo, Ningbo 315100, China
3 Department of Chemistry, University College London (UCL), 20 Gordon Street, London WC1H 0AJ, UK; yiyangliu0904@163.com
4 National Engineering Laboratory of Cleaner Hydrometallurgical Production Technology, Institute of Process Engineering, Chinese Academy of Sciences, Beijing 100190, China; wangys@ipe.ac.cn (Y.W.); yanggang@ipe.ac.cn (G.Y.)
5 School of Engineering, Edith Cowan University, 270 Joondalup Drive, Joondalup, WA 6027, Australia
* Correspondence: huan.jin@nottingham.edu.cn (H.J.); jun.he@nottingham.edu.cn (J.H.); yong.sun@nottingham.edu.cn (Y.S.)

Citation: Lian, Z.; Wang, Y.; Zhang, X.; Yusuf, A.; Famiyeh, L.; Murindababisha, D.; Jin, H.; Liu, Y.; He, J.; Wang, Y.; et al. Hydrogen Production by Fluidized Bed Reactors: A Quantitative Perspective Using the Supervised Machine Learning Approach. *J* **2021**, *4*, 266–287. https://doi.org/10.3390/j4030022

Academic Editors: Said Elnashaie, Hatem Harraz and Arian Ebneyamini

Received: 16 June 2021
Accepted: 2 July 2021
Published: 7 July 2021

Abstract: The current hydrogen generation technologies, especially biomass gasification using fluidized bed reactors (FBRs), were rigorously reviewed. There are involute operational parameters in a fluidized bed gasifier that determine the anticipated outcomes for hydrogen production purposes. However, limited reviews are present that link these parametric conditions with the corresponding performances based on experimental data collection. Using the constructed artificial neural networks (ANNs) as the supervised machine learning algorithm for data training, the operational parameters from 52 literature reports were utilized to perform both the qualitative and quantitative assessments of the performance, such as the hydrogen yield (HY), hydrogen content (HC) and carbon conversion efficiency (CCE). Seven types of operational parameters, including the steam-to-biomass ratio (SBR), equivalent ratio (ER), temperature, particle size of the feedstock, residence time, lower heating value (LHV) and carbon content (CC), were closely investigated. Six binary parameters have been identified to be statistically significant to the performance parameters (hydrogen yield (HY)), hydrogen content (HC) and carbon conversion efficiency (CCE) by analysis of variance (ANOVA). The optimal operational conditions derived from the machine leaning were recommended according to the needs of the outcomes. This review may provide helpful insights for researchers to comprehensively consider the operational conditions in order to achieve high hydrogen production using fluidized bed reactors during biomass gasification.

Keywords: hydrogen; fluidized bed reactor; supervised machine learning; review

1. Introduction

The United Nations (UN) has promoted climate neutrality to produce no net greenhouse gas (GHG) emissions for years, as GHG emission has been considered one of the major causes of global warming [1]. GHG emissions in the atmosphere from fossil fuels, generated either by power plants or automobiles, have also risen and become a tremendous threat to environmental sustainability [2,3]. In recent years, a series of efforts shas been made, including using renewable resources or clean energy such as hydrogen fuels to mitigate the situation, reducing carbon dioxide emissions and in realizing sustainable

development [4–7]. However, the conventional generation techniques of hydrogen are adopted from fossil fuels, including steam methane reforming (SMR) and derivations from natural gas, also known as "gray hydrogen" [8]. On a related note, hydrogen production using renewable resources is called "blue hydrogen" or biohydrogen (such as by the means of electrolysis, nuclear, solar photovoltaic-PV, wind, hydro or geothermal technologies), which is regarded as more environmentally friendly [3,5,6,9–13]. The current hydrogen generation technologies from different feedstocks are summarized in Figure 1. Apparently, the balance of feedstock between deploying fossil fuel and renewable resources for hydrogen generation has become lopsided, and this trend will become more prominent in the foreseeable future.

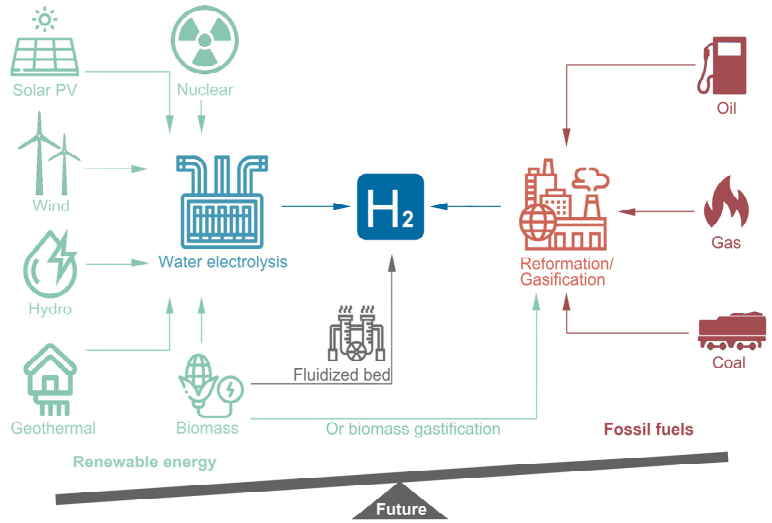

Figure 1. Hydrogen production from different resources via different technical routes. Left: blue hydrogen. Right: gray hydrogen.

While a large number of techniques are available for hydrogen generation, the employment of those techniques faces great challenges when it comes to considering the more complex factors (e.g., cost-effectiveness, reliability and efficiency). For example, electrolysis is considered to be not cost-effective, and bioprocessing through dark fermentation using biomass as the feedstock is not efficient due to its intrinsic, slow biological processing feature [14]. Recently, biomass gasification by fluidized bed reactors (FBRs) has been found to significantly enhance the efficiency of hydrogen production, but its obvious drawbacks, such as complex reaction mechanisms and catalyst usage, somehow limit its application [15,16]. For fluidized bed operation, many operational parameters (such as the carbon content, residence time, lower heating values and particle size) play vital roles in determining the expected outcomes (e.g., conversions and yield) [17], and there are very few examples in the literature that try to systematically correlate these critical operational parameters with the corresponding performances. Therefore, this initiates our interest in using our developed artificial neural networks, coupled with a response surface methodology (ANNs-RSM) algorithm, to assess the statistical significance of the investigated operational parameters upon the performances of FBRs during hydrogen generation. The quantitative assessment of reported references for hydrogen generation from different FBRs, to the best of our knowledge, has not been reported before.

2. Analysis Approach

2.1. Literature Collections and Scoping

In this review, the literature utilized was primarily collected through keyword searches in scientific data bases including Science Direct, Web of Science and Google Scholar. The keyword combinations used in the academic search tool were primarily set as "fluidized bed", "hydrogen production" and "biomass gasification". To keep up with the most recent

research in this field, selected literature were restricted within the last five years, from 2016 to 2021, in five main subject areas (energy, chemical engineering, chemistry, material science and environmental sciences). As shown in Figure 2, besides 2018, the total number of publications in hydrogen generation from FBRs experienced a steady increase from 2016 to 2020. Among the subject areas, energy (En) related research accounts for up to 40% of the total publications each year, indicating great research potential and applications in the field. Chemical engineering (CE) contributes around 20% of the total publications, while other areas individually account for about 10%. The total number of publications in the last three years (2019–2021) also experience a steady increase, indicating an increased research interest in this field.

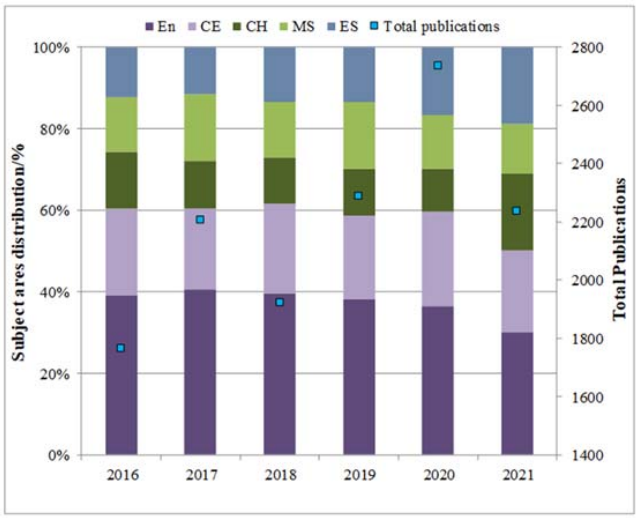

Figure 2. Summary of publication from Scopus for hydrogen generation by subject areas, where En refers to energy, CE refers to chemical engineering, CH refers to chemistry, MS refers to material science, and ES refers to environmental sciences.

2.2. Methodology for Data Training and Predictions

Artificial neural network (ANN) is a well-developed soft computing technique. Inspired by the human neurological system, ANN is constructed in layers, and information is fed forward to these layers. The configuration of the networks adopts 10 × 10 nodes (two hidden layers) feed forward progression using Gaussian as the transformation function, which is often widely adopted as a supervised machine learning configuration setup [18]. In this work, 52 collected references with seven inputs (namely temperature, residence time, equivalent ratio, steam-to-biomass ratio, carbon content, lower heating value, and particle size) and three outputs (hydrogen yield, hydrogen content, and carbon conversion efficiency) were used as a training data set. The cross-out validation technique was deployed, and the mean square error (MSE) and mean absolute relative residuals (MARR) were computed as:

$$\mathrm{MSE}\% = \frac{1}{N_{sam}} \sum_{j=1}^{N_{sam}} \left(r \left| i^{sam} - r_i^{cal} \right| \right)^2 \times 100\% \quad (1)$$

$$\mathrm{MARR}\% = \frac{1}{N_{sam}} \sum_{j=1}^{N_{exp}} \left(\frac{\left| r_i^{sam} - r_i^{cal} \right|}{r_i^{sam}} \right) \times 100\% \quad (2)$$

where N_{sam} refers to the number of data set, and i^{sam} and r_i^{cal} are actual and prediction number, respectively. The acceptable uncertainties are ±10%. The response surface methodology (RSM) was used for data matrix generation, and the corresponding outputs were produced from ANNs via data training. The detailed data handling and algorithm specifica-

tions can be found from our previously reported works [18–20]. After the completion of the supervised data learning, analysis of variation (ANOVA) using commercial Design Expert® Version 11 software package (Stat-Ease, Inc., Minneapolis, MN, USA) was deployed for statistical analysis.

3. Source of Hydrogen

3.1. Steam Methane Reforming (SMR)

Currently, approximately 95% of the world's hydrogen is derived from fossil fuels through such processes as natural gas steam reforming, coal gasification, and petroleum refining. Chemical processing allows the transformation of hydrocarbon fuels to hydrogen under various conditions. The most common pathway to produce hydrogen in the industry is natural gas reforming, also known as steam methane reforming (SMR) [21–23]. This is an endothermic process that applies high-temperature steam to convert methane into carbon dioxide and hydrogen. Methane enters the reactor as feedstock, mixing and reacting with water to form carbon monoxide and hydrogen in the temperature and pressure range of 700 to 1000 °C and 3–25 bar, respectively, in the presence of a catalyst [24,25]. Meanwhile, the formed carbon monoxide is shifted with steam to produce carbon dioxide and extra hydrogen through a process known as the water–gas shift (WGS) reaction.

$$\text{SMR: } CH_4 + H_2O \leftrightarrow CO + 3H_2;\ \Delta H298 = 206 \text{ kJ mol}^{-1} \quad (3)$$

$$\text{WGS: } CO + H_2O \leftrightarrow CO_2 + H_2;\ \Delta H298 = -41 \text{ kJ mol}^{-1} \quad (4)$$

The overall reaction is expressed as follows:

$$CH_4 + 2H_2O \leftrightarrow CO_2 + 4H_2;\ \Delta H298 = 165 \text{ kJ mol}^{-1} \quad (5)$$

Despite achieving the desired conversion, the final products may contain an excessive amount of carbon dioxide, which necessitates further separation, using techniques such as pressure swing adsorption, to purify the hydrogen-rich syngas [24]. On an industrial scale, SMR can achieve the highest hydrogen production efficiency compared to other techniques. Notwithstanding the well-established SMR technology, thermochemical conversion techniques such as auto-thermal reforming, partial oxidation, and plasma catalytic reforming were developed and applied by researchers for efficient hydrogen generation [23,26–28]. However, most of the abovementioned thermochemical processes mainly use fossil fuels, generate greenhouse gas emissions, and consume a considerable amount of energy, especially when combined with carbon capture process. The other two important technologies, electrolysis and biomass gasification for hydrogen production, were reviewed in the following section, and a comparison of these three technologies were summarized in Table 1.

3.2. Electrolysis

Electrolysis is a hydrogen production approach that dissociates hydrogen from water by applying an induced electric current from an electrolyzer. It is an endothermic reaction, meaning that energy input (electricity) is required during the process. Electrolysis technique is clean, as it only generates hydrogen and oxygen from water molecules without any other harmful emissions [29,30]. The overall splitting reaction that occurs in the electrolysis cell, within the electrolyzer, is demonstrated in Equation (6):

$$2H_2O \rightarrow 2H_2 + O_2 \quad (6)$$

Ionic reactions take place at the two electrodes (anode and cathode) within the electrolysis cell, which are connected through electrolytes. At present, the commonly used electrolytes are alkaline, acidic or salt solutions. In an acidic cell, water molecules are primarily converted to oxygen and positively charged protons at the anode. The protons subsequently move forward to the cathode through the electrolyte, whilst electrons are

transported to the cathode through an external circuit (such as a direct current). Finally, protons and electrons react at the cathode to form hydrogen gas in the presence of a catalyst [31]. This process can be described by the following equations:

$$\text{Anode reaction: } 2H_2O \rightarrow 4H^+ + O_2 + 4e^- \quad (7)$$

$$\text{Cathode reaction: } 2H^+ + 2e^- \rightarrow H_2 \quad (8)$$

In the case of an alkaline electrolyte, the electric potential drives the negative hydroxide ions toward the anode and the positive protons to the cathode to form hydrogen gas, as shown below [32]:

$$\text{Anode reaction: } 4OH^- \rightarrow 2H_2O + O_2 + 4e^- \quad (9)$$

$$\text{Cathode reaction: } 2H_2O + 2e^- \rightarrow H_2 + 2OH^- \quad (10)$$

Among the three electrolytic media, the alkaline electrolyte is more desirable considering potential corrosion or spoilage of some metal electrodes in acidic electrolyte, as well as the possible undesired by-product generation in a salt solution. Recent studies explored many other harsh challenges such as high working temperature and molten hydroxides, the optimized working conditions and the reaction mechanism, to fill the gaps in reference electrodes for hydrogen production under high temperature electrolyte conditions [33,34]. Apart from the conventional options, novel alternatives such as proton exchange membrane (PEM) electrolyzer technology, alkaline anion exchange membrane (AAEM), and solid oxide water electrolysis (SOWE), etc., are well-developed [35–38]. Unfortunately, their excessive cost could hinder their large-scale application in hydrogen production, especially, the use of precious metal catalysts including iridium, ruthenium, palladium and platinum during PEM electrolysis [39]. Apart from that, costly electrode materials and high energy consumption also impede the widely application of water electrolysis in large commercial plants. On the other hand, although electrolysis is regarded as a clean process, it could be indirectly associated with carbon emissions if the electricity input is sourced from fossil fuels combustion, unless the "green" electricity comes from renewable sources such as wind or solar energy [40]. Overall, electrolysis can be a promising method for clean hydrogen production, but it has not yet been recognized as cost-effective and widely deployed compared to fossil fuels. Its future development should be focused on the exploitation of inexpensive catalysts and materials, higher productivity, and usage of larger amounts of affordable and renewable electricity [41,42].

Table 1. Comparisons of hydrogen production technologies by steam methane reforming, electrolysis and biomass gasification.

Production Technology	Feedstock	Processes Involved	Overall Reactions	Efficiency	Advantages	Limitations	References
Steam Methane Reforming	Methane and steam	• Reforming of steam and methane • Water–gas shift	$CH_4 + 2H_2O \leftrightarrow CO_2 + 4H_2$	70–85%	• Mature commercially available technology • Highest hydrogen production efficiency	• Use of fossil fuels or refinery byproducts cause GHG emission • Additional heat transfer units	[21–25]
Electrolysis	Water and electricity	• Ionic reactions	$2H_2O \rightarrow 2H_2 + O_2$; $2H_2O \rightarrow 4H^+ + O_2 + 4e^-$; $2H^+ + 2e^- \rightarrow H_2$ *	50–70%	• Abundant water and electricity sources • No GHG emission and other by-products unless fossil fuels used as electricity source	• Expensive catalyst and materials • Corrosion of electrodes	[29–32,35]
Biomass gasification	Biomass	• Pyrolysis • Char gasification, carbon residues combustion • Tar cracking or reforming	Biomass + Air/oxygen/steam $\rightarrow H_2 + CO + CO_2 + (N_2) + CH_4 +$ Tar + Char + Hydrocarbons	35–55%	• Abundant and renewable resources • Carbon neutral • Cost-effective	• Thermodynamic equilibrium and other byproducts • Relatively low efficiency	[43–47]

* Here, only acidic electrolyte case is shown as a demonstration.

3.3. Gasification of Biomass

Biomass is an abundant renewable organic resource that incorporates forest residues (such as wood logs, straw), agricultural residues (such as cornstalk, rice husk), municipal wastes (such as sewage slurry), biological residues (such as shells), etc. [48–50]. Recently, there is an ever-increasing attention on bioenergy due to its low cost, versatile applications and carbon neutrality [50]. Biomass can be directly used as combustion fuels or upgraded as a feedstock through a variety of methods including thermal conversions (such as gasification, pyrolysis and torrefaction) [49,51,52], chemical conversions (such as Fischer–Tropsch synthesis which converts biomass-based products into a synthetic lubrication oil and synthetic fuel) [53–56], biological conversions (such as fermentation, composting, anaerobic digestion) [57–59], electrochemical conversions (such as electrocatalytic oxidation), etc. [60]. Among such numerus pathways, biomass gasification, as a matured technology either commercially or pilot scale demonstration, has been intensively explored for converting organic materials to hydrogen and other products.

Gasification is a highly endothermic process that includes a series of reactions such as pyrolysis, char gasification, carbon residues combustion, and tar cracking or reforming. Biomass gasification implements biomass as feedstock, operating at high temperatures (700 to 1000 °C) with an oxidizing agent (air/oxygen/steam) supply to produce hydrogen, carbon monoxide, carbon dioxide, and other products such as char, tar, nitrogen, methane, etc. [47]. The produced syngas can be transported to power plants for power and electricity generation or used as a chemical feedstock for processes such as methanol production. A typical air gasification reaction of biomass can be expressed as:

$$\text{Biomass} + \text{Air} \rightarrow H_2 + CO + CO_2 + N_2 + CH_4 + \text{Tar} + \text{Char} + \text{Hydrocarbons} \quad (11)$$

Due to the non-combustible nitrogen content of air and incomplete reaction, the hydrogen production efficiency of the air gasifier is generally lower than oxygen and steam gasifiers. Although the hydrogen content of oxygen gasification is enriched, the use of pure oxygen is commercially uneconomical. The steam gasification is a viable pathway of treating biomass and has the highest conversion efficiency of the three oxidizing agents, which is around 53 to 55 vol% of H_2 production, whereas that of air gasification is around 8 to 10 vol% [61]. Additionally, the carbon-to-hydrogen mass ratio can be reduced through water–gas shift reaction, which further increases the hydrogen content and calorific value of the yield gases:

$$\text{Biomass} + \text{steam} \rightarrow H_2 + CO + CO_2 + \text{tar} + \text{char} \quad (12)$$

Water–gas shift reaction converts carbon monoxide to more hydrogen:

$$CO + H_2O \rightarrow H_2 + CO_2 \quad (13)$$

Biomass gasification is versatile for adapting various types of biomass in terms of producing hydrogen and syngas. However, the process is limited by thermodynamic equilibrium and undesired products such as tar, coupled with other challenges such as types of gasification reactors, use of catalyst, operating parameters, etc. [44,62]. Typical gasification reactors are classified as entrained flow gasifiers (EFG), fixed bed gasifiers (FXBG) and fluidized bed gasifiers (FBG), as illustrated in Figure 3. In an EFG as shown in Figure 3A, biomass can be fed at the top with the gasifying agent (downflow system) or the bottom through side burners (upflow system). Normally, biomass is heated in a temperature range of 1200 to 2000 °C at 20 to 70 bar, during which particles travel with oxygen and steam along the reactor in a very short residence time [63]. Since the gas flow velocity in the system is high enough, both the biomass fuels and the formed synthesis gas are entrained in the same flow direction. Meanwhile, the high temperature and pressure can result in almost complete reaction that high quality of synthesis gas can be obtained. Most importantly, the high temperature ensures a full destruction of the undesired volatile

components such as tar. However, it is challenging that a pre-treatment of the biomass fuel is required to ensure unhindered flow and stable heat and mass transfer during the reaction [63]. The fuels must be dried and milled into finely ground particles with size diameter of hundred micrometers before it can be introduced to the systems. Nevertheless, due to different source and the intrinsic physical properties of biomass, the particle-stated biomass fuels still suffer from poor mobility with flows. This may lead to insufficient mixing, and therefore restrict the overall efficiency. Besides, the operating temperature is beyond the ash fusion temperature and slagging could be a challenging issue in the system. In addition, keeping a high flow demands large oxidant input into the system [63,64].

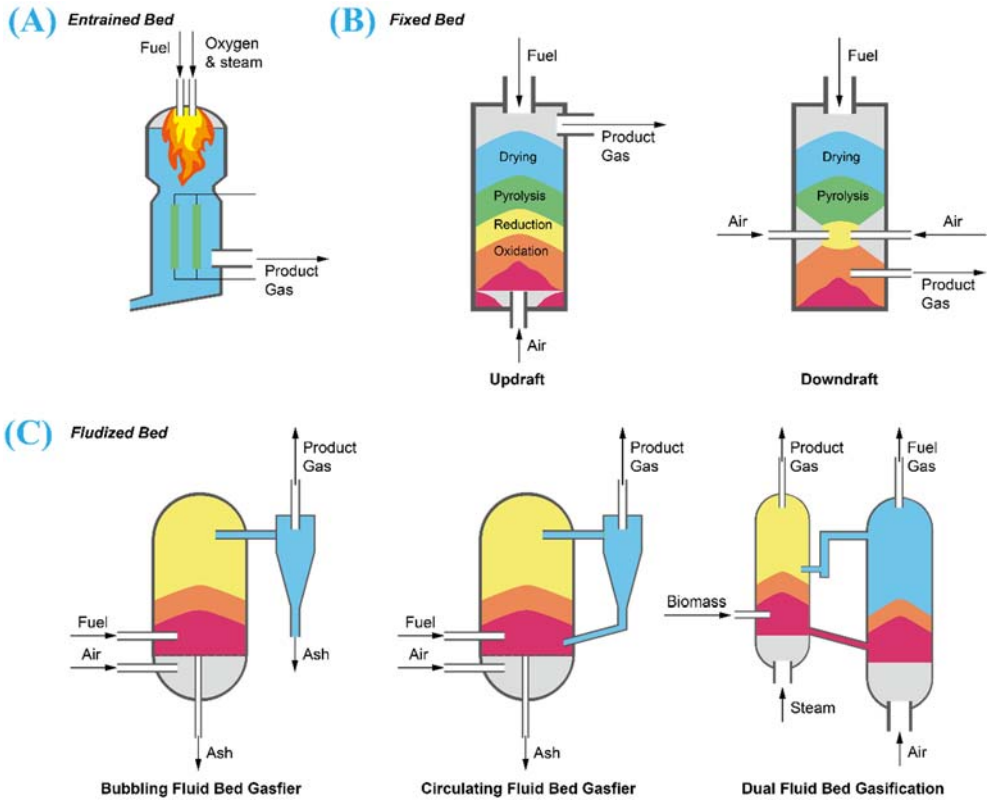

Figure 3. Schematic illustration of different types of gasifiers: (**A**) entrained flow, (**B**) fixed bed (left: updraft and right: downdraft) and (**C**) Fluidized bed (left: bubbling fluidized bed, middle: circulating fluidized bed and right: dual fluidized bed).

Fixed bed gasifier has a bed of solid fuel particles in a cylindrical space, as demonstrated in Figure 3B. FXBGs normally operate in a temperature range of 300 to 1000 °C without extra pressure exerted to the system. FXBGs are categorized into updraft and downdraft types. In these configurations, the gasification agent enters the reactor in different directions [45,65]. In updraft FXBG (see Figure 3B), the biomass fuel is introduced from the top entrance and the gasification agent (steam and oxygen) from the bottom of the reactor. The biomass descends through the bed while being heated and converted to synthesis gas. The gasification process includes drying, pyrolysis, reduction, and oxidation, after which the synthesis gas leaves the gasifier through the top exit. Hydrogen content produced by the updraft FXBG is higher than EFG, but contains higher fractions of tar (10 to 20 g/m^3) and a huge amount of other pyrolysis products, which need to be removed before further utilization [65]. For downdraft FXBGs, the reactor through an inlet and the targeted syngas is separated from the bottom, as shown in Figure 3B. The downdraft FXBGs can enable hydrocarbon cracking and depressing tar content [43,45]. However, downdraft FXBGs usually have a lower gas yield than upward FXBGs and are therefore limited to upscaling for commercial production. Overall, although fixed bed gasifiers produce cleaner

product gas, relative high tar content and low conversion rate severely limit FXBGS to small scale applications [43,65].

Owing to excellent solid–gas contact and promising heat and mass transfer, fluidized bed gasifiers exhibit better performance for biomass gasification than EFGs and FXBGs. FBGs are viable to deal with a variety of types and sizes of biomass and have great potential to scale up for commercial applications [66]. In a fluidized bed, the biomass is introduced above a dense fluid bed (typically quartz sand or catalytic particles) and upward flow of gasification reactants, supplied to the bottom of the gasifier, serve as fluidizing medium. The bed operating temperature is normally within a range of 700 to 1000 °C, which is below the ash fusion or softening point to avoid ash agglomeration and blockage or defluidization of the bed [66,67]. Biomass settles to the hot bed surface and is heated rapidly, enabling drying and pyrolysis to take place. The uniform high temperature profile maintained in FBGs is beneficial for achieving a high carbon conversion efficiency and reduction of tar and light hydrocarbons. Meanwhile, constant fluidization facilitates continuous and proper mixing between the oxidant and biomass particles, promoting a high reaction efficiency. However, char combustion under such temperature partly restricts gasification process and negatively impacts the entire process. In addition, tar formation is the main barrier towards higher yield of synthesis gas [68,69].

Fluidized gasification reactors are operated in three modes including bubbling, circulating, and dual beds, as depicted in Figure 3C. In a bubbling fluidized bed (BFB), the fuel is introduced from the bottom or side of the bed. The bed starts bubbling when the velocity of gasification agent is beyond the minimum fluidization velocity. The product syngas is extracted from the top of the reactor and cleaned in a cyclone, as shown in Figure 3C. BFB demonstrates capability to treat high-moisture biomass, but significant instability in the presence of bubbling and rising gas channeling [70,71]. Circulating fluidized bed (CFB) features two operating units, which are a fast velocity riser reactor and a circulating loop cyclone (Figure 3C middle). In this concept, biomass is treated under a higher gas velocity (superficial flow velocity) than BFB in a more drastic fluidization state. A mixture of product syngas and bed particles rise to the top and separated in cyclones, where the issued-out solids recirculate into a riser from the bottom. Therefore, greater overall efficiency could be realized through the looping design [46]. Dual fluidized bed (DFB) systems or two-stage fluidized bed systems comprise of two fluidized bed reactors interlinked with a solid looping configuration, as illustrated in Figure 3C (right) [72]. They can be a combination of two BFBs, two CFBs or a BFB and a CFB. The two connected fluidized beds are independently accountable for pyrolysis and combustion reactions [73]. In the combustion chamber, air and fuels are fed in and solid reactants are heated and combusted. Consequently, combustion turns flue gas, at the top of reactor, into a connected cyclone, after which the bed materials are transported to the second FBG. Biomass gasification takes place with the help of a hot bed material and steam to produce syngas gas and char. Later, the bed material and char are transferred back to the first FBG for char combustion, repeating the previous steps. By this means, the two processes do not interfere with each other, and high conversion efficiency is ensured [72,74]. Table 2 summarizes different types of gasifiers for biomass gasification, as well as their operational conditions, advantages and limitations.

Table 2. Comparison of different types of gasifiers for biomass gasification including their operational conditions, advantages and limitations.

Gasifier Types	Design Configurations	Descriptions	T (°C)	P (bar)	Advantages	Limitations	References
Entrained flow	Upflow system	• Biomass fed at the bottom with the gasifying agent • Syngas exits from the top	1000–1400	25–30	• High quality of synthesis gas • Elimination of tar • Short residence time	• High gas flow velocity, high temperature and pressure, large oxidant demand • High energy consumption • Complex pretreatment	[63,64]
	Downflow system	• Biomass fed at the top with the gasifying agent • Syngas exits from the bottom	1200–2000	20–70			
Fixed bed	Updraft	• Biomass fed at the top and gasifying agent from the bottom of reactors • Syngas exits from the top	300–1000	Atmospheric pressure	• Higher gas yield	• Higher fractions of tar and other byproducts	[45,65]
	Downdraft	• Biomass fed at the top and gasifying agent from the middle of reactors • Syngas exits from the bottom	300–1000	Atmospheric pressure	• Hydrocarbon cracking and limited tar content	• Lower gas yield • tar formation and other byproducts	[43,45]
Fluidized bed	Bubbling	• Biomass fed at the bottom or side and gasifying agent from the bottom of reactors • Syngas exits from the bottom	700–1000	1–35	• Capable of treating high moisture biomass • Uniform high temperature profile • Betting mixing • High carbon conversion efficiency • No ash agglomeration	• Tar formation and other byproducts	[75–79]
	Circulating	• Biomass fed to the bed and gasifying agent from the bottom of reactors • Syngas exits from the top and partially recycled from cyclone and sent back to gasifier	700–1000	1–20	• Capable of treating high moisture biomass • Uniform high temperature profile • Better mixing • High carbon conversion efficiency • No ash agglomeration	• Extra operating units	[46,80–83]
	Dual	• Two operation units combined pyrolysis and combustion	700–1000	1–35	• Higher working efficiency • Flexible and independent working units • Char removal	• Higher energy demand • Extra operating units	[84–89]

4. Statistical Analysis of Parameter upon Output

In this review, among the different operational parameters, we choose seven parameters (temperature, residence time, equivalent ratio, steam-to-biomass ratio, carbon content, lower heating value and particle size) due to availability in reported literatures. Taking the feedstock sources for an example, different sources of feedstock may own various calorific values, carbon content, or moisture content that can significantly affect the conversion rate to hydrogen. The results are summarized in Tables 3 and 4 (Table 3 for different types of FBGs and Table 4 for general FBGs that the types were not specified in the literatures). Using the collected references as training data set via ANNs-RSM algorithm, the predictions were made against the actual reported values from references. The results are shown in Figure 4. Apart from some values possessing relative higher uncertainties over ±20%, the majority of calculated data fall into the reasonable range, indicating that our constructed network can generate reliable predictions.

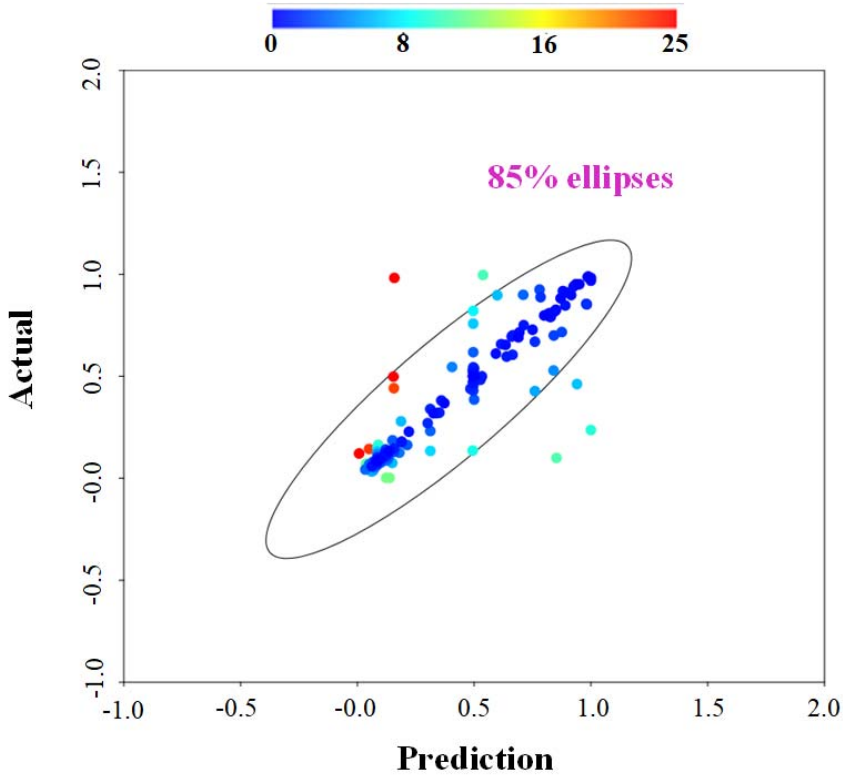

Figure 4. Analysis result—actual versus prediction from ANNs modeling, where color bar represents the uncertainties.

The types of fluidized bed reactors and their corresponding reported hydrogen contents from Tables 3 and 4 were summarized and plotted in Figure 5. Obviously, different types of fluidized bed reactors from different reported sources tend to yield different reported values of hydrogen contents. In Figure 5, the top three reported hydrogen contents were annotated. For example, the hydrogen content could reach nearly 80% when almond shell was fed into fluidized bed gasifier using commercial nickel as catalyst. The bubbling fluidized bed reactor also generated hydrogen content reaching around 70% when empty fruit bunch was used as feedstock.

Table 3. Operational parameters versus corresponding hydrogen generation, where - represents the value that is not available from the literature (in this work, for easiness of data handling, the voids were replaced by the average reported value).

Bed Type	Feedstock	Feedstock Particle Size (μm)	Carbon Content (wt.%)	LHV (MJ/Nm^3)	T/°C	Process Time/min	ER	SBR	Yield (Nm^3/kg)	Yield H_2 Content/vol%	(CCE) %	Reference
Bubbling	Torrefied and raw pine	468	13.80	-	800	45	0.28	-	80.56	15.13	-	[75]
	Wood sawdust	1500	-	-	850	300	-	-	1.15	42.00	85.00	[76]
	Rice husk	7500	11.69	3.84	600	-	0.20	-	0.50	2.70	95.00	[77]
	Wood-PET pellets	6000	12.16	19.19	800	90	0.28	-	-	8.10	98.60	[90]
	Rice husk	-	36.00	9.30	800	60	0.30	-	-	12.50	-	[91]
	MSW	-	8.46	14.40	900	-	0.25	1.00	-	-	-	[92]
	Cocoa shells	461	21.70	-	900	60	0.23	1.20	1.49	49.10	50.00	[71]
	Rice husk and coal	1575	22.37	-	850	210	0.26	1.21	-	8.64	89.00	[78]
	Pine sawdust	-	12.60	-	600	120	-	0.20	1.03	38.60	71.20	[93]
	-	-	-	14.30	800	42	0.30	-	-	4.00	76.00	[94]
	Pine sawdust and brown coal	4000	13.20	-	900	-	0.20	0.50	-	50.60	84.20	[79]
	Torrefied woodchips	240	22.82	19.26	850	30	0.22	1.20	1.12	28.66	89.20	[95]
	Carbonaceous feedstock	15,000	11.50	20.53	785	30	0.21	-	2.10	7.10	84.10	[96]
	Rice husk	-	14.99	-	850	-	0.30	0.80	-	11.00	76.00	[97]
	Cypress wood chips	-	20.64	15.80	700	-	0.30	1.20	-	0.59	-	[98]
	Torrefied woodchips	-	20.18	3.00	800	30	0.24	-	1.77	14.31	78.00	[99]
	Poultry litter	525	22.82	19.26	850	90	-	1.40	1.41	43.00	87.52	[100]
	-	310	8.81	5.36	700	30	0.30	0.24	1.36	17.58	88.00	[101]
	Spruce slice	615	-	20.05	809	60	0.20	-	-	9.69	50.00	[102]
	Miscanthus	300	14.99	4.25	850	-	0.35	0.50	-	12.30	-	[103]
	Torrefied and raw pine	630	-	5.55	915	60	0.32	-	-	10.80	91.00	[104]
Circulating	Torrefied wood residues and mixed wood	5000	24.65	11.70	850	180	0.22	1.26	1.60	53.00	82.40	[83]
	Wood residue and Tabas coal	175	18.20	-	850	55	0.40	-	-	52.70	-	[46]
	Methane and biomass	-	-	-	1000	-	0.21	1.00	-	28.00	-	[81]
	Sub-bituminous coal and sawdust	3675	35.93	22.39	800	-	0.29	-	2.11	12.63	84.00	[80]
	-	1890	-	3.96	800	-	0.41	0.60	-	4.00	-	[82]
Dual	PP plastic pellets, wood chips and plant capsules	660	8.01	26.00	900	10.67	0.30	-	2.53	29.70	82.00	[85]
	Rice straw	1250	18.74	-	800	120	0.24	-	1.20	5.38	84.77	[86]
	PE plastic bags, sawdust and PP plastic particles	780	5.00	-	900	-	0.30	0.50	-	53.10	-	[87]
	PE plastic bags, sawdust and PP plastic particles	780	5.00	-	700	35	0.30	0.60	-	39.38	-	[88]
	Volatile, fixed carbon and ash	-	17.16	9.90	800	-	0.19	1.56	1.72	32.34	91.50	[84]
	Pine sawdust	200	12.73	11.40	850	120	-	0.30	10.51	47.30	64.00	[89]
	Biomass briquette	-	18.71	11.00	670	300	0.19	-	1.20	24.00	98.82	[105]
	PE plastic bags, wood chips and PP particles	660	-	-	900	35	0.30	0.60	-	50.96	92.59	[106]

Table 4. Operational parameters of general fluidized bed (types not specified in literatures) versus corresponding hydrogen generation, where - represents the value that is not available from the literature (in this work, for easiness of data handling, the voids were replaced by the average reported value).

Catalyst	Feedstock	Feedstock Particle Size (μm)	Carbon Content (wt.%)	LHV (MJ/Nm^3)	T/°C	Process Time/min	ER	SBR	Yield (Nm^3/kg)	Yield H_2 Content/vol%	CCE %	References
ZSM-5 zeolite	Beech-wood and poly	-	-	-	854	90	0.30	0.63	-	-	98.20	[107]
-	Palm kernel shell and sub-bituminous coal	160	40.00	21.13	800	1440	0.60	0.20	-	12.00	82.80	[108]
NiO/modified dolomite	Coffee husk	-	-	-	900	-	0.15	1.50	1.75	27.00	-	[109]
-	Carbonaceous feedstock	275	0.80	-	820	-	0.19	1.00	2.00	40.00	-	[110]
-	Citrus peel	500	40.31	4.65	750	20	0.30	1.25	0.69	26.00	87.00	[111]
$Ni/CeO_2/Al_2CO_3$	Wood residue	-	49.18	-	823	44	0.17	0.71	1.66	42.52	93.56	[112]
-	Straw	7500	17.15	14.96	850	60	0.16	-	0.90	17.00	75.00	[113]
Commercial Ni-catalyst *1	Almond shells	-	11.00	-	815	60	-	0.49	1.70	55.30	-	[114]
Ternary molten carbonates	Forestry biomass waste	-	3.89	-	750	60	-	1.00	-	55.00	-	[115]
-	Pine sawdust and MSW	2000	18.82	-	850	-	0.21	-	13.40	9.80	-	[69]
High-alumina bauxite	Straw	7500	17.50	9.35	726	60	0.16	-	-	14.90	70.99	[116]
Calcium (Ca)	Rice husk and bamboo dust	670	-	5.05	800	30	0.35	0.41	1.72	-	98.00	[117]
Commercial Zeolite *2	Empty fruit bunch	3000	8.60	-	973	30	-	2.00	-	75.00	-	[118]
Industrial sludge derived catalysts	-	320	10.35	4.84	800	50	0.30	1.00	-	12.46	100.00	[67]
SCG ash	-	1400	20.00	12.20	900	30	-	0.53	-	6.00	-	[119]
Coal bottom ash	Palm kernel shell	750	14.25	12.50	692	60	-	1.50	-	79.77	59.90	[120]
Calcined dolomite	-	5000	35.20	-	1000	50	0.14	1.00	-	49.10	60.80	[121]

Company information: *1 Johnson Matthey. *2 Zeolyst, Malaysia Sdn. Bhd., Malaysia.

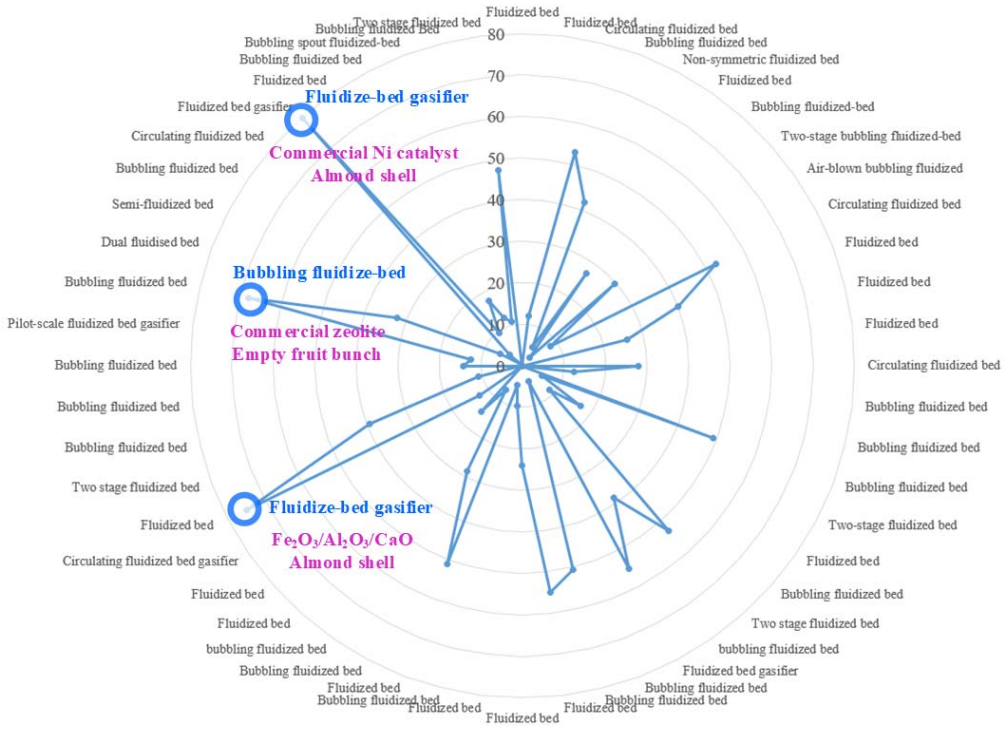

Figure 5. Types of fluidized bed versus hydrogen yield (vol-%), the circles with number labelled represent hydrogen yield (%) and the top three hydrogen yield case are displayed in blue and purple.

The statistical analysis of the impact of seven process parameters on the corresponding three outputs using ANOVA are shown in Figure 6. In this work, instead of investigating the statistical significance of singular process parameters upon the responses, we mainly focused on statistical significance of the binary combined parameters upon those three responses, which is often more meaningful from a practical operation point of view. Among all the investigated binary combined parameters (total $7 \times 6 = 42$ different combinations, see Figure 6A), six binary combined parameters (Figure 6B) were identified and found to be statistically significant to the response.

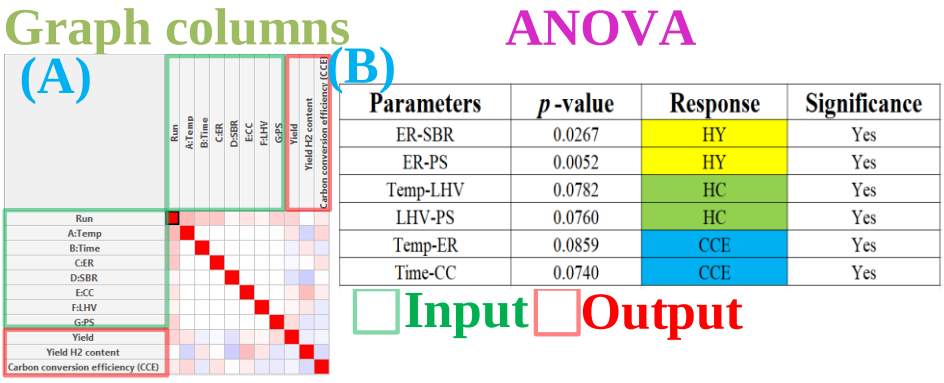

Parameters	*p*-value	Response	Significance
ER-SBR	0.0267	HY	Yes
ER-PS	0.0052	HY	Yes
Temp-LHV	0.0782	HC	Yes
LHV-PS	0.0760	HC	Yes
Temp-ER	0.0859	CCE	Yes
Time-CC	0.0740	CCE	Yes

Figure 6. Statistical analysis for the impact of process parameters upon responses, (**A**) graph column of parameters and responses, (**B**) ANOVA of all parameters towards the responses, where HY represents hydrogen yield, HC refers to hydrogen content, and CCE refers to carbon conversion efficiency (%), SBR refers to steam-to-biomass ratio (-), ER refers to equivalence ratio, LHV refers to lower heating value (MJ/Nm^3), CC refers to carbon content (%), PS refers to particle size (μm) and Temp refers to temperature (°C).

The statistical analysis of the impact of the binary combined factors on responses are shown in Figure 7. Figure 7A shows the steam-to-biomass ratio (SBR) and equivalence ratio (ER) versus hydrogen yield (HY). SBR refers to the ratio between steam content and biomass fed to the gasifier, and ER represents the actual air-to-biomass ratio with respect to stoichiometry for complete combustion [88,113]. Both SBR and ER are significant parameters that need to be maintained at optimal values in order to achieve relatively high HY. High HY values were found at both high SBR and ER regions in Figure 7A. It can be explained that a higher value of SBR (i.e., 1.5–2.0) tends to increase HY on account of the water–gas shift reactions. Meanwhile, higher ER (above 0.5) indicates the availability of more oxidizing agent in the system, which enhances the oxidation reaction. It also maintains continuous tar cracking and eventually boosts the total amount of producer gas, although HY does not experience significant growth [113]. It should be noted that both SBR and ER should not go beyond a limit (mentioned above) because more oxidizing agent in the gasifier would lead to incomplete gasification and an increase in carbon-contained gases, leading to adverse effect on HY. In addition, both high values could result in more energy and material consumption. Interestingly, high HY is also found in the region of lower SBR and ER values. For example, reduction of ER to a range within 0.2 to 0.3 facilitates hydrogen production and other gaseous content. However, low ER below 0.15 (Figure 7A) can leave a proportion of unconverted char and tar in the system. If SBR is too low, a deficiency of the water–gas shift process would likewise restrict the final HY. Figure 7B demonstrates the particle size (PS) and ER against HY. It is suggested that under a low ER, small feedstock particle size (e.g., 3000 μm) enriches HY, as large surface area favors efficient heat transfer during gasification. Conversely, larger sized biomass feedstock suffers from poor thermal decomposition, leading to high volatile content, which in return produces high tar content and low HY [122]. Figure 7C depicts the influence of residence time (Time) and temperature (Temp) on hydrogen content (HC) in the producer gas. Although the results suggested that longer residence time (such as 1500 min) also leads to higher HC, it is regarded as inefficient considering factors such as a noticeable amount of energy, material input, and other economic considerations. On the other hand, adequate residence time should be ensured, as both temperature and reactions need certain periods to attain steady state. This corresponds to the predictions in Figure 7C that the optimal residence time is controlled within 180 min. Conversely, higher temperatures intensify HC values due to the intrinsic endothermic process of hydrogen production and a decrease in carbon monoxide. However, it is also dependent on the moisture content of the feedstock, as part of the energy would be consumed during drying. Therefore, lower temperature may impede effective processing of biomass with high moisture content [123]. Nevertheless, the char combustion demands extra energy input at high temperature conditions, i.e., over 850 °C, where HC is limited under this circumstance. As for lower heating value (LHV), there is an increasing trend of HC directly associated with larger LHV of biomass fuels, as shown in Figure 7D. This suggests that favor high LHV of the feedstock favors HC at any instance. Carbon conversion efficiency (CCE) is determined by the mass of carbon in producer gas over the mass of carbon in biomass feedstock. A High CCE value implies high hydrogen to carbon monoxide ratio as well as high tar conversion [124]. The analysis results, as illustrated in Figure 7F, shows the estimated optimal CCE values fall within the ER and temperature range of $0.15 < ER < 0.35$ and 700 to 850 °C, respectively. Restricting the residence time within 180 min, a high CCE can be achieved by selecting biomass with a wide range of carbon content (CC) over 8%, as seen in Figure 7F. Overall, the parametric factors surveyed above have a joint influence on hydrogen production and a rough prediction can be made based on those given values. Therefore, this may serve as a guide for users when considering hydrogen production from biomass using fluidized bed gasifiers.

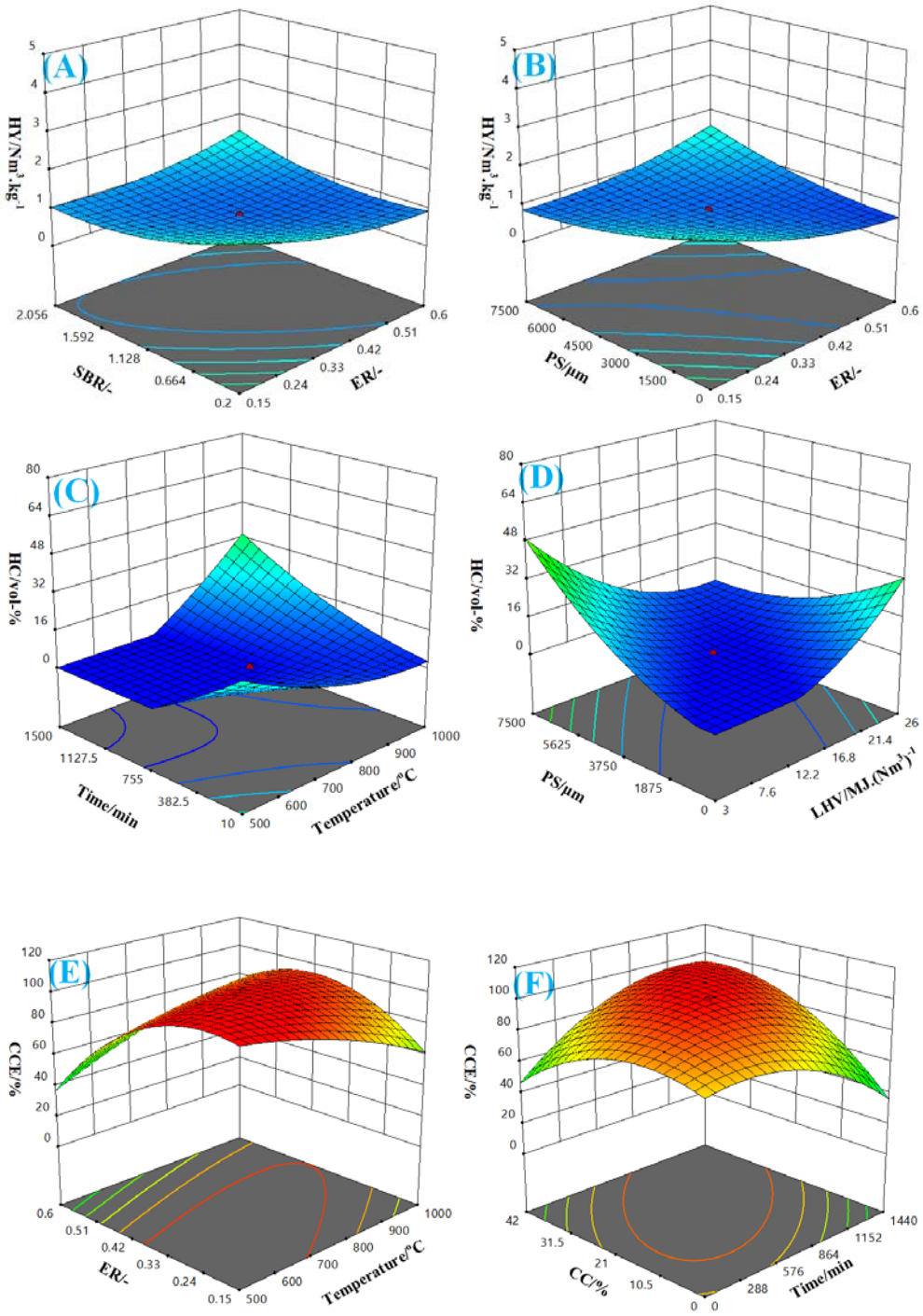

Figure 7. Statistical analysis for the impact of process parameters upon responses, (**A**) SBR-ER-HY, (**B**) PS-ER-HY, (**C**) Time-Temp-HC, (**D**) PS-LHV-HC, (**E**) ER-Temp-CCE and (**F**) CC-Time-CCE.

5. Conclusions

In this paper, the commonly used hydrogen production technologies including steam methane reforming, electrolysis, and biomass gasification were reviewed and compared. Among the mentioned technologies, biomass gasification using fluidized bed reactor was thoroughly reviewed, including the types and operating conditions. Biomass gasification can be considered as a promising alternative technology for hydrogen production owing to the renewable, abundant, carbon neutral, and cost-effective nature of the feedstock. Subsequently, biomass gasifiers including entrained flow gasifier, fixed bed and fluidized

bed reactor (FBR) were compared. Due to the inherent advantage of enhanced mass and heat transfer, the FBR was identified as the most promising biomass gasification technique for hydrogen production. In addition, to quantitatively assess the pivotal operational parameters of FBR, seven key inputs and three outputs were extracted from the reported literatures as a training data set. These inputs are SBR, ER, temperature, PS of feedstock, residence time, LHV, and CC. The three outputs are HY, HC, and CCE. The results of the statistical analysis indicate that six binary parameters are statistically significant to the outputs. In terms of high HY, SBR, and ER, relatively low values were suggested for efficient reaction and economic considerations. A high HC was proposed based on a shorter reaction time within 180 min under 850 °C for biomass that contained high LHV and fine particle sizes. The optimal CCE values could be obtained within an ER range of 0.15 to 0.35, operating temperature of 700 to 850 °C, reaction time within 180 min, and with CC values beyond 8%, as inputs. This analysis may provide a revealing insight for users who wish to realize high working efficiency using biomass gasification technology for hydrogen production. However, besides the parametric conditions mentioned in the content, other essential factors such as the types and amount of catalyst were not assessed in this paper. This is because currently, the data could not be quantified as an effective data input to the analysis system. Therefore, both the qualitative and quantitative evaluation of this factor will be conducted in our future study.

Author Contributions: Z.L.: drafting, writing and analysis; Y.W. (Yixiao Wang): data curation; X.Z.: data curation; A.Y.: writing; L.F.: writing and drafting; D.M.: writing and drafting; H.J.: programming and supervision; Y.L.: writing and supervision; J.H.: supervision; Y.W. (Yunshan Wang): project management; G.Y.: project management; Y.S.: writing, supervision and project management. All authors have read and agreed to the published version of the manuscript.

Funding: Funding was acquired through the University of Nottingham Ningbo China (FoSE New Researchers Grant I01210100011), the Faculty Inspiration Grant of University of Nottingham (FIG2019), the Qianjiang Talent Scheme (QJD1803014), the National Key R&D Program of China (Grant: 2018YFC1903500), the Ningbo Science and Technology Innovation 2025 Key Project (Grant 2020Z100) and the Ningbo Municipal Commonweal Key Program (Grant 2019C10033 and 2019C10104).

Institutional Review Board Statement: Not applicable.

Informed Consent Statement: Not applicable.

Data Availability Statement: Not applicable.

Acknowledgments: The authors also sincerely appreciate the critical and insightful comments raised by those anonymous reviewers for significantly improving the quality of this work.

Conflicts of Interest: The authors declare no conflict of interest.

Abbreviations

AAEM	Alkaline anion exchange membrane
ANNs	Artificial neural networks
ANNs-RSM	Artificial neural networks coupled with response surface methodology
ANOVA	Analysis of variation
BFB	Bubbling fluidized bed
CC	Carbon content
CCE	Carbon conversion efficiency
CE	Chemical engineering
CFB	Circulating fluidized bed
CH	Chemistry
DFB	Dual fluidized bed
En	Energy
ES	Environmental sciences
FBG	Fluidized bed gasifiers
FBR	Fluidized bed reactors

EFG	Entrained flow gasifiers
ER	Equivalence ratio
FXBG	Fixed bed gasifiers
GHG	Greenhouse gas
HC	Hydrogen content
HY	Hydrogen yield
i^{sam}	Actual
LHV	Lower heating value
MARR	Mean absolute relative residuals
MS	Material science
MSE	Mean square error
N_{sam}	Number of data set
PEM	Proton exchange membrane
PS	Particle size
r_i^{cal}	Prediction
RSM	Response surface methodology
SBR	Steam-to-biomass ratio
SMR	Steam methane reforming
SOWE	Solid oxide water electrolysis
Temp	Temperature
UN	United Nations
WGS	Water-gas shift

References

1. Sun, Y.; Lin, Z.; Peng, S.H.; Sage, V.; Sun, Z. A Critical Perspective on CO2 Conversions into Chemicals and Fuels. *J. Nanosci. Nanotechnol.* **2019**, *19*, 3097–3109. [CrossRef]
2. Schlapbach, L.; Zuttel, A. Hydrogen-storage materials for mobile applications. *Nature* **2001**, *414*, 353–358. [CrossRef]
3. Sun, Y.; Zhang, J.; Yang, G.; Li, Z. Analysis of trace elements in corncob by microwave Digestion-ICP-AES. *Spectrosc. Spect. Anal.* **2007**, *27*, 1424–1427.
4. Sun, Y.; He, J.; Yang, G.; Sun, G.; Sage, V. A Review of the Enhancement of Bio-Hydrogen Generation by Chemicals Addition. *Catalysts* **2019**, *9*, 353. [CrossRef]
5. Al-Juboori, O.; Sher, F.; Khalid, U.; Niazi, M.B.K.; Chen, G.Z. Electrochemical Production of Sustainable Hydrocarbon Fuels from CO2 Co-electrolysis in Eutectic Molten Melts. *ACS Sustain. Chem. Eng.* **2020**, *8*, 12877–12890. [CrossRef]
6. Al-Juboori, O.; Sher, F.; Hazafa, A.; Khan, M.K.; Chen, G.Z. The effect of variable operating parameters for hydrocarbon fuel formation from CO2 by molten salts electrolysis. *J. CO2 Util.* **2020**, *40*, 101193. [CrossRef]
7. Sun, Y.; Mang, J.P.; Yang, G.; Li, Z.H. Study on the spectra of spruce lignin with chlorine dioxide oxidation. *Spectrosc. Spect. Anal.* **2007**, *27*, 1551–1554.
8. Mallapaty, S. How China Could Be Carbon Neutral by Mid-Century. *Nature* **2020**, *586*, 482–483. [CrossRef] [PubMed]
9. YLiu, Y.; Min, J.L.; Feng, X.Y.; He, Y.; Liu, J.Z.; Wang, Y.X.; He, J.; Do, H.N.; Sage, V.; Yang, G.; et al. A Review of Biohydrogen Productions from Lignocellulosic Precursor via Dark Fermentation: Perspective on Hydrolysate Composition and Electron-Equivalent Balance. *Energies* **2020**, *13*, 1–27.
10. Sun, Y.; Wang, Y.S.; Yang, G.; Sun, Z. Optimization of biohydrogen production using acid pretreated corn stover hydrolysate followed by nickel nanoparticle addition. *Int. J. Energy Res.* **2020**, *44*, 1843–1857. [CrossRef]
11. Sun, Y.; Zhang, J.; Yang, G.; Li, Z. Analysis of trace elements in corn by inductively coupled plasma-atomic emission spectrometry. *Food Sci.* **2007**, *28*, 236–237.
12. Al-Shara, N.K.; Sher, F.; Yaqoob, A.; Chen, G.Z. Electrochemical investigation of novel reference electrode Ni/Ni(OH)$_2$ in comparison with silver and platinum inert quasi-reference electrodes for electrolysis in eutectic molten hydroxide. *Int. J. Hydrogen Energy* **2019**, *44*, 27224–27236. [CrossRef]
13. Al-Shara, N.K.; Sher, F.; Iqbal, S.Z.; Sajid, Z.; Chen, G.Z. Electrochemical study of different membrane materials for the fabrication of stable, reproducible and reusable reference electrode. *J. Energy Chem.* **2020**, *49*, 33–41. [CrossRef]
14. Sun, Y.; Yang, G.; Zhang, J.P.; Wen, C.; Sun, Z. Optimization and kinetic modeling of an enhanced bio-hydrogen fermentation with the addition of synergistic biochar and nickel nanoparticle. *Int. J. Energy Res.* **2019**, *43*, 983–999. [CrossRef]
15. Martínez, I.; Grasa, G.; Meyer, J.; Di Felice, L.; Kazi, S.; Sanz, C.; Maury, D.; Voisin, C. Performance and operating limits of a sorbent-catalyst system for sorption-enhanced reforming (SER) in a fluidized bed reactor. *Chem. Eng. Sci.* **2019**, *205*, 94–105. [CrossRef]
16. Di Giuliano, A.; Giancaterino, F.; Courson, C.; Foscolo, P.U.; Gallucci, K. Development of a Ni-CaO-mayenite combined sorbent-catalyst material for multicycle sorption enhanced steam methane reforming. *Fuel* **2018**, *234*, 687–699. [CrossRef]
17. Sun, Y.; Zhang, J.P.; Yang, G.; Li, Z.H. An improved process for preparing activated carbon with large specific surface area from corncob. *Chem. Biochem. Eng. Q.* **2007**, *21*, 169–174.

18. Sun, Y.; Yang, G.; Xu, M.; Xu, J.; Sun, Z. A simple coupled ANNs-RSM approach in modeling product distribution of Fischer-Tropsch synthesis using a microchannel reactor with Ru-promoted Co/Al_2O_3 catalyst. *Int. J. Energy Res.* **2019**, *44*, 1046–1061. [CrossRef]
19. Wang, Y.S.; Yang, G.; Sage, V.; Xu, J.; Sun, G.Z.; He, J.; Sun, Y. Optimization of dark fermentation for biohydrogen production using a hybrid artificial neural network (ANN) and response surface methodology (RSM) approach. *Environ. Prog. Sustain. Energy* **2020**. [CrossRef]
20. Sun, Y.; Yang, G.; Wen, C.; Zhang, L.; Sun, Z. Artificial neural networks with response surface methodology for optimization of selective CO2 hydrogenation using K-promoted iron catalyst in a microchannel reactor. *J. CO2 Util.* **2018**, *24*, 10–21. [CrossRef]
21. Wang, M.; Tan, X.; Motuzas, J.; Li, J.; Liu, S. Hydrogen production by methane steam reforming using metallic nickel hollow fiber membranes. *J. Membr. Sci.* **2021**, *620*, 118909. [CrossRef]
22. Meloni, E.; Martino, M.; Ricca, A.; Palma, V. Ultracompact methane steam reforming reactor based on microwaves susceptible structured catalysts for distributed hydrogen production. *Int. J. Hydrogen Energy* **2021**, *46*, 13729–13747. [CrossRef]
23. Zhu, X.; Liu, X.; Lian, H.-Y.; Liu, J.-L.; Li, X.-S. Plasma catalytic steam methane reforming for distributed hydrogen production. *Catal. Today* **2019**, *337*, 69–75. [CrossRef]
24. Wu, H.-C.; Rui, Z.; Lin, J.Y.S. Hydrogen production with carbon dioxide capture by dual-phase ceramic-carbonate membrane reactor via steam reforming of methane. *J. Membr. Sci.* **2020**, *598*, 117780. [CrossRef]
25. Noh, Y.S.; Lee, K.-Y.; Moon, D.J. Hydrogen production by steam reforming of methane over nickel based structured catalysts supported on calcium aluminate modified SiC. *Int. J. Hydrogen Energy* **2019**, *44*, 21010–21019. [CrossRef]
26. Xu, F.; Wang, Y.-m.; Li, F.; Nie, X.-y.; Zhu, L.-H. Hydrogen production by the steam reforming and partial oxidation of methane under the dielectric barrierdischarge. *J. Fuel Chem. Technol.* **2021**, *49*, 367–373. [CrossRef]
27. Araújo, P.M.; da Costa, K.M.; Passos, F.B. Hydrogen production from methane autothermal reforming over CaTiO3, BaTiO3 and SrTiO3 supported nickel catalysts. *Int. J. Hydrogen Energy* **2021**, *46*, 24107–24116. [CrossRef]
28. Lian, H.-Y.; Liu, J.-L.; Li, X.-S.; Zhu, X.; Weber, A.Z.; Zhu, A.-M. Plasma chain catalytic reforming of methanol for on-board hydrogen production. *Chem. Eng. J.* **2019**, *369*, 245–252. [CrossRef]
29. Nguyen, T.; Abdin, Z.; Holm, T.; Mérida, W. Grid-connected hydrogen production via large-scale water electrolysis. *Energy Convers. Manag.* **2019**, *200*, 112108. [CrossRef]
30. Zhang, C.; Greenblatt, J.B.; Wei, M.; Eichman, J.; Saxena, S.; Muratori, M.; Guerra, O.J. Flexible grid-based electrolysis hydrogen production for fuel cell vehicles reduces costs and greenhouse gas emissions. *Appl. Energy* **2020**, *278*, 115651. [CrossRef]
31. Purnami, N.; Hamidi, M.N.; Sasongko, D.; Widhiyanuriyawan, I.N.G. Wardana, Strengthening external magnetic fields with activated carbon graphene for increasing hydrogen production in water electrolysis. *Int. J. Hydrogen Energy* **2020**, *45*, 19370–19380. [CrossRef]
32. Avci, A.C.; Toklu, E. A new analysis of two phase flow on hydrogen production from water electrolysis. *Int. J. Hydrogen Energy* **2021**. [CrossRef]
33. Al-Shara, N.K.; Sher, F.; Iqbal, S.Z.; Curnick, O.; Chen, G.Z. Design and optimization of electrochemical cell potential for hydrogen gas production. *J. Energy Chem.* **2021**, *52*, 421–427. [CrossRef]
34. Sher, F.; Al-Shara, N.K.; Iqbal, S.Z.; Jahan, Z.; Chen, G.Z. Enhancing hydrogen production from steam electrolysis in molten hydroxides via selection of non-precious metal electrodes. *Int. J. Hydrogen Energy* **2020**, *45*, 28260–28271. [CrossRef]
35. Ju, H.; Giddey, S.; Badwal, S.P.S. Role of iron species as mediator in a PEM based carbon-water co-electrolysis for cost-effective hydrogen production. *Int. J. Hydrogen Energy* **2018**, *43*, 9144–9152. [CrossRef]
36. Kumar, S.S.; Ramakrishna, S.U.B.; Krishna, S.V.; Srilatha, K.; Devi, B.R.; Himabindu, V. Synthesis of titanium (IV) oxide composite membrane for hydrogen production through alkaline water electrolysis. *S. Afr. J. Chem. Eng.* **2018**, *25*, 54–61.
37. Wang, L.; Chen, M.; Küngas, R.; Lin, T.-E.; Diethelm, S.; Maréchal, F.; Van Herle, J. Power-to-fuels via solid-oxide electrolyzer: Operating window and techno-economics. *Renew. Sustain. Energy Rev.* **2019**, *110*, 174–187. [CrossRef]
38. Faid, A.Y.; Barnett, A.O.; Seland, F.; Sunde, S. NiCu mixed metal oxide catalyst for alkaline hydrogen evolution in anion exchange membrane water electrolysis. *Electrochim. Acta* **2021**, *371*, 137837. [CrossRef]
39. Bhavanari, M.; Lee, K.-R.; Tseng, C.-J.; Tang, I.H.; Chen, H.-H. CuFe electrocatalyst for hydrogen evolution reaction in alkaline electrolysis. *Int. J. Hydrogen Energy* **2021**. [CrossRef]
40. Gutiérrez-Martín, F.; Amodio, L.; Pagano, M. Hydrogen production by water electrolysis and off-grid solar PV. *Int. J. Hydrogen Energy* **2020**. [CrossRef]
41. Kakoulaki, G.; Kougias, I.; Taylor, N.; Dolci, F.; Moya, J.; Jäger-Waldau, A. Green hydrogen in Europe—A regional assessment: Substituting existing production with electrolysis powered by renewables. *Energy Convers. Manag.* **2020**, *228*, 113649. [CrossRef]
42. Holm, T.; Borsboom-Hanson, T.; Herrera, O.E.; Mérida, W. Hydrogen costs from water electrolysis at high temperature and pressure. *Energy Convers. Manag.* **2021**, *237*, 114106. [CrossRef]
43. Aydin, E.S.; Yucel, O.; Sadikoglu, H. Experimental study on hydrogen-rich syngas production via gasification of pine cone particles and wood pellets in a fixed bed downdraft gasifier. *Int. J. Hydrogen Energy* **2019**, *44*, 17389–17396. [CrossRef]
44. Chianese, S.; Fail, S.; Binder, M.; Rauch, R.; Hofbauer, H.; Molino, A.; Blasi, A.; Musmarra, D. Experimental investigations of hydrogen production from CO catalytic conversion of tar rich syngas by biomass gasification. *Catal. Today* **2016**, *277*, 182–191. [CrossRef]

45. Jahromi, R.; Rezaei, M.; Samadi, S.H.; Jahromi, H. Biomass gasification in a downdraft fixed-bed gasifier: Optimization of operating conditions. *Chem. Eng. Sci.* **2021**, *231*, 116249. [CrossRef]
46. Peng, W.-X.; Ge, S.-B.; Ebadi, A.G.; Hisoriev, H.; Esfahani, M.J. Syngas production by catalytic co-gasification of coal-biomass blends in a circulating fluidized bed gasifier. *J. Clean. Prod.* **2017**, *168*, 1513–1517. [CrossRef]
47. Xiao, Y.; Xu, S.; Song, Y.; Shan, Y.; Wang, C.; Wang, G. Biomass steam gasification for hydrogen-rich gas production in a decoupled dual loop gasification system. *Fuel Process. Technol.* **2017**, *165*, 54–61. [CrossRef]
48. Anniwaer, A.; Chaihad, N.; Zhang, M.; Wang, C.; Yu, T.; Kasai, Y.; Abudula, A.; Guan, G. Hydrogen-rich gas production from steam co-gasification of banana peel with agricultural residues and woody biomass. *Waste Manag.* **2021**, *125*, 204–214. [CrossRef]
49. Li, C.; Liu, R.; Zheng, J.; Wang, Z.; Zhang, Y. Production of hydrogen-rich syngas from absorption-enhanced steam gasification of biomass with conch shell-based absorbents. *Int. J. Hydrogen Energy* **2021**. [CrossRef]
50. Posso, F.; Siguencia, J.; Narváez, R. Residual biomass-based hydrogen production: Potential and possible uses in Ecuador. *Int. J. Hydrogen Energy* **2020**, *45*, 13717–13725. [CrossRef]
51. Li, S.; Zheng, H.; Zheng, Y.; Tian, J.; Jing, T.; Chang, J.-S.; Ho, S.-H. Recent advances in hydrogen production by thermo-catalytic conversion of biomass. *Int. J. Hydrogen Energy* **2019**, *44*, 14266–14278. [CrossRef]
52. Yang, S.; Chen, L.; Sun, L.; Xie, X.; Zhao, B.; Si, H.; Zhang, X.; Hua, D. Novel Ni–Al nanosheet catalyst with homogeneously embedded nickel nanoparticles for hydrogen-rich syngas production from biomass pyrolysis. *Int. J. Hydrogen Energy* **2021**, *46*, 1762–1776. [CrossRef]
53. Tomasek, S.; Lónyi, F.; Valyon, J.; Hancsók, J. Fuel purpose hydrocracking of biomass based Fischer-Tropsch paraffin mixtures on bifunctional catalysts. *Energy Convers. Manag.* **2020**, *213*, 112775. [CrossRef]
54. Sun, Y.; Wang, Y.X.; He, J.; Yusuf, A.; Wang, Y.X.; Yang, G.; Xiao, X. Comprehensive kinetic model for acetylene pretreated mesoporous silica supported bimetallic Co-Ni catalyst during Fischer-Tropsch synthesis. *Chem. Eng. Sci.* **2021**. [CrossRef]
55. Sun, Y.; Jia, Z.; Yang, G.; Zhang, L.; Sun, Z. Fischer-Tropsch synthesis using iron based catalyst in a microchannel reactor: Performance evaluation and kinetic modeling. *Int. J. Hydrogen Energy* **2017**, *42*, 29222–29235. [CrossRef]
56. Sun, Y.; Yang, G.; Zhang, L.; Sun, Z. Fischer-Tropsch synthesis in a microchannel reactor using mesoporous silica supported bimetallic Co-Ni catalyst: Process optimization and kinetic modeling. *Chem. Eng. Process.* **2017**, *119*, 44–61. [CrossRef]
57. Batista, A.P.; Gouveia, L.; Marques, P.A.S.S. Fermentative hydrogen production from microalgal biomass by a single strain of bacterium Enterobacter aerogenes—Effect of operational conditions and fermentation kinetics. *Renew. Energy* **2018**, *119*, 203–209. [CrossRef]
58. Sugiarto, Y.; Sunyoto, N.M.S.; Zhu, M.; Jones, I.; Zhang, D. Effect of biochar in enhancing hydrogen production by mesophilic anaerobic digestion of food wastes: The role of minerals. *Int. J. Hydrogen Energy* **2021**, *46*, 3695–3703. [CrossRef]
59. Khan, I. Waste to biogas through anaerobic digestion: Hydrogen production potential in the developing world—A case of Bangladesh. *Int. J. Hydrogen Energy* **2020**, *45*, 15951–15962. [CrossRef]
60. Yang, C.; Wang, C.; Zhou, L.; Duan, W.; Song, Y.; Zhang, F.; Zhen, Y.; Zhang, J.; Bao, W.; Lu, Y.; et al. Refining d-band center in Ni0.85Se by Mo doping: A strategy for boosting hydrogen generation via coupling electrocatalytic oxidation 5-hydroxymethylfurfural. *Chem. Eng. J.* **2021**, *422*, 130125. [CrossRef]
61. Situmorang, Y.A.; Zhao, Z.; An, P.; Yu, T.; Rizkiana, J.; Abudula, A.; Guan, G. A novel system of biomass-based hydrogen production by combining steam bio-oil reforming and chemical looping process. *Appl. Energy* **2020**, *268*, 115122. [CrossRef]
62. Moneti, M.; Di Carlo, A.; Bocci, E.; Foscolo, P.U.; Villarini, M.; Carlini, M. Influence of the main gasifier parameters on a real system for hydrogen production from biomass. *Int. J. Hydrogen Energy* **2016**, *41*, 11965–11973. [CrossRef]
63. Dhanavath, K.N.; Shah, K.; Islam, M.S.; Ronte, A.; Parthasarathy, R.; Bhargava, S.K.; Bankupalli, S. Experimental investigations on entrained flow gasification of Torrefied Karanja Press Seed Cake. *J. Environ. Chem. Eng.* **2018**, *6*, 1242–1249. [CrossRef]
64. Schneider, J.; Grube, C.; Herrmann, A.; Rönsch, S. Atmospheric entrained-flow gasification of biomass and lignite for decentralized applications. *Fuel Process. Technol.* **2016**, *152*, 72–82. [CrossRef]
65. Yao, X.; Zhao, Z.; Chen, S.; Zhou, H.; Xu, K. Migration and transformation behaviours of ash residues from a typical fixed-bed gasification station for biomass syngas production in China. *Energy* **2020**, *201*, 117646. [CrossRef]
66. Marcantonio, V.; De Falco, M.; Capocelli, M.; Bocci, E.; Colantoni, A.; Villarini, M. Process analysis of hydrogen production from biomass gasification in fluidized bed reactor with different separation systems. *Int. J. Hydrogen Energy* **2019**, *44*, 10350–10360. [CrossRef]
67. Chen, Y.-H.; Ngo, T.N.L.T.; Chiang, K.-Y. Enhanced hydrogen production in co-gasification of sewage sludge and industrial wastewater sludge by a pilot-scale fluidized bed gasifier. *Int. J. Hydrogen Energy* **2021**, *46*, 14083–14095. [CrossRef]
68. Butera, G.; Gadsbøll, R.Ø.; Ravenni, G.; Ahrenfeldt, J.; Henriksen, U.B.; Clausen, L.R. Thermodynamic analysis of methanol synthesis combining straw gasification and electrolysis via the low temperature circulating fluid bed gasifier and a char bed gas cleaning unit. *Energy* **2020**, *199*, 117405. [CrossRef]
69. Cao, Y.; Fu, L.; Mofrad, A. Combined-gasification of biomass and municipal solid waste in a fluidized bed gasifier. *J. Energy Inst.* **2019**, *92*, 1683–1688. [CrossRef]
70. Nam, H.; Wang, S.; Sanjeev, K.C.; Seo, M.W.; Adhikari, S.; Shakya, R.; Lee, D.; Shanmugam, S.R. Enriched hydrogen production over air and air-steam fluidized bed gasification in a bubbling fluidized bed reactor with CaO: Effects of biomass and bed material catalyst. *Energy Convers. Manag.* **2020**, *225*, 113408. [CrossRef]

71. González-Vázquez, M.P.; García, R.; Gil, M.V.; Pevida, C.; Rubiera, F. Comparison of the gasification performance of multiple biomass types in a bubbling fluidized bed. *Energy Convers. Manag.* **2018**, *176*, 309–323. [CrossRef]
72. Yaghoubi, E.; Xiong, Q.; Doranehgard, M.H.; Yeganeh, M.M.; Shahriari, G.; Bidabadi, M. The effect of different operational parameters on hydrogen rich syngas production from biomass gasification in a dual fluidized bed gasifier. *Chem. Eng. Processing-Process Intensif.* **2018**, *126*, 210–221. [CrossRef]
73. Jeong, Y.-S.; Choi, Y.-K.; Kang, B.-S.; Ryu, J.-H.; Kim, H.-S.; Kang, M.-S.; Ryu, L.-H.; Kim, J.-S. Lab-scale and pilot-scale two-stage gasification of biomass using active carbon for production of hydrogen-rich and low-tar producer gas. *Fuel Process. Technol.* **2020**, *198*, 106240. [CrossRef]
74. Hanchate, N.; Malhotra, R.; Mathpati, C.S. Design of experiments and analysis of dual fluidized bed gasifier for syngas production: Cold flow studies. *Int. J. Hydrogen Energy* **2021**, *46*, 4776–4787. [CrossRef]
75. Kulkarni, A.; Baker, R.; Abdoulmomine, N.; Adhikari, S.; Bhavnani, S. Experimental study of torrefied pine as a gasification fuel using a bubbling fluidized bed gasifier. *Renew. Energy* **2016**, *93*, 460–468. [CrossRef]
76. Valin, S.; Bedel, L.; Guillaudeau, J.; Thiery, S.; Ravel, S. CO2 as a substitute of steam or inert transport gas in a fluidised bed for biomass gasification. *Fuel* **2016**, *177*, 288–295. [CrossRef]
77. Kook, J.W.; Choi, H.M.; Kim, B.H.; Ra, H.W.; Yoon, S.J.; Mun, T.Y.; Kim, J.H.; Kim, Y.K.; Lee, J.G.; Seo, M.W. Gasification and tar removal characteristics of rice husk in a bubbling fluidized bed reactor. *Fuel* **2016**, *181*, 942–950. [CrossRef]
78. Bharath, M.; Raghavan, V.; Prasad, B.V.S.S.S.; Chakravarthy, S.R. Co-gasification of Indian rice husk and Indian coal with high-ash in bubbling fluidized bed gasification reactor. *Appl. Therm. Eng.* **2018**, *137*, 608–615. [CrossRef]
79. Ma, X.; Zhao, X.; Gu, J.; Shi, J. Co-gasification of coal and biomass blends using dolomite and olivine as catalysts. *Renew. Energy* **2019**, *132*, 509–514. [CrossRef]
80. Mallick, D.; Mahanta, P.; Moholkar, V.S. Co–gasification of coal/biomass blends in 50 kWe circulating fluidized bed gasifier. *J. Energy Inst.* **2020**, *93*, 99–111. [CrossRef]
81. Nakyai, T.; Authayanun, S.; Patcharavorachot, Y.; Arpornwichanop, A.; Assabumrungrat, S.; Saebea, D. Exergoeconomics of hydrogen production from biomass air-steam gasification with methane co-feeding. *Energy Convers. Manag.* **2017**, *140*, 228–239. [CrossRef]
82. Wan, Z.; Hu, J.; Qi, X. Numerical analysis of hydrodynamics and thermochemical property of biomass gasification in a pilot-scale circulating fluidized bed. *Energy* **2021**, *225*, 120254. [CrossRef]
83. Di Marcello, M.; Tsalidis, G.A.; Spinelli, G.; de Jong, W.; Kiel, J.H.A. Pilot scale steam-oxygen CFB gasification of commercial torrefied wood pellets. The effect of torrefaction on the gasification performance. *Biomass Bioenergy* **2017**, *105*, 411–420. [CrossRef]
84. Cao, Y.; Bai, Y.; Du, J. Air-steam gasification of biomass based on a multi-composition multi-step kinetic model: A clean strategy for hydrogen-enriched syngas production. *Sci. Total Environ.* **2021**, *753*, 141690. [CrossRef]
85. Liu, Z.-S.; Lin, C.-L.; Chang, T.-J.; Weng, W.-C. Waste-gasification efficiency of a two-stage fluidized-bed gasification system. *Waste Manag.* **2016**, *48*, 250–256. [CrossRef]
86. Liu, L.; Huang, Y.; Cao, J.; Liu, C.; Dong, L.; Xu, L.; Zha, J. Experimental study of biomass gasification with oxygen-enriched air in fluidized bed gasifier. *Sci. Total. Environ.* **2018**, *626*, 423–433. [CrossRef]
87. Lin, C.-L.; Wu, M.-H.; Weng, W.-C. Effect of the type of bed material in two-stage fluidized bed gasification reactors on hydrogen gas synthesis and heavy metal distribution. *Int. J. Hydrogen Energy* **2019**, *44*, 5633–5639. [CrossRef]
88. Kuo, J.-H.; Lin, C.-L.; Ho, C.-Y. Effect of fluidization/gasification parameters on hydrogen generation in syngas during fluidized-bed gasification process. *Int. J. Hydrogen Energy* **2021**. [CrossRef]
89. Wang, G.; Xu, S.; Wang, C.; Zhang, J. Biomass Gasification and Hot Gas Upgrading in a Decoupled Dual-Loop Gasifier. *Energy Fuels* **2017**, *31*, 8181–8192. [CrossRef]
90. Robinson, T.; Bronson, B.; Gogolek, P.; Mehrani, P. Comparison of the air-blown bubbling fluidized bed gasification of wood and wood–PET pellets. *Fuel* **2016**, *178*, 263–271. [CrossRef]
91. Manatura, K.; Lu, J.-H.; Wu, K.-T.; Hsu, H.-T. Exergy analysis on torrefied rice husk pellet in fluidized bed gasification. *Appl. Therm. Eng.* **2017**, *111*, 1016–1024. [CrossRef]
92. Couto, N.; Silva, V.; Cardoso, J.; Rouboa, A. 2nd law analysis of Portuguese municipal solid waste gasification using CO2/air mixtures. *J. CO2 Util.* **2017**, *20*, 347–356. [CrossRef]
93. Zhang, J.; Wang, M.; Xu, S.; Feng, Y. Hydrogen and methane mixture from biomass gasification coupled with catalytic tar reforming, methanation and adsorption enhanced reforming. *Fuel Process. Technol.* **2019**, *192*, 147–153. [CrossRef]
94. Hervy, M.; Remy, D.; Dufour, A.; Mauviel, G. Air-blown gasification of Solid Recovered Fuels (SRFs) in lab-scale bubbling fluidized-bed: Influence of the operating conditions and of the SRF composition. *Energy Convers. Manag.* **2019**, *181*, 584–592. [CrossRef]
95. Nguyen, N.M.; Alobaid, F.; May, J.; Peters, J.; Epple, B. Experimental study on steam gasification of torrefied woodchips in a bubbling fluidized bed reactor. *Energy* **2020**, *202*, 117744. [CrossRef]
96. Pio, D.T.; Tarelho, L.A.C.; Tavares, A.M.A.; Matos, M.A.A.; Silva, V. Co-gasification of refused derived fuel and biomass in a pilot-scale bubbling fluidized bed reactor. *Energy Convers. Manag.* **2020**, *206*, 112476. [CrossRef]
97. Gupta, S.; Choudhary, S.; Kumar, S.; De, S. Large eddy simulation of biomass gasification in a bubbling fluidized bed based on the multiphase particle-in-cell method. *Renew. Energy* **2021**, *163*, 1455–1466. [CrossRef]

98. Kartal, F.; Özveren, U. A comparative study for biomass gasification in bubbling bed gasifier using Aspen HYSYS. *Bioresour. Technol. Rep.* **2021**, *13*, 100615. [CrossRef]
99. Porcu, A.; Xu, Y.; Mureddu, M.; Dessì, F.; Shahnam, M.; Rogers, W.A.; Sastri, B.S.; Pettinau, A. Experimental validation of a multiphase flow model of a lab-scale fluidized-bed gasification unit. *Appl. Energy* **2021**, *293*, 116933. [CrossRef]
100. Nguyen, N.M.; Alobaid, F.; Epple, B. Chemical looping gasification of torrefied woodchips in a bubbling fluidized bed test rig using iron-based oxygen carriers. *Renew. Energy* **2021**, *172*, 34–45. [CrossRef]
101. Pandey, D.S.; Kwapinska, M.; Gómez-Barea, A.; Horvat, A.; Fryda, L.E.; Rabou, L.P.L.M.; Leahy, J.J.; Kwapinski, W. Poultry Litter Gasification in a Fluidized Bed Reactor: Effects of Gasifying Agent and Limestone Addition. *Energy Fuels* **2016**, *30*, 3085–3096. [CrossRef]
102. Agu, C.E.; Moldestad, B.M.E.; Pfeifer, C. Assessment of Combustion and Gasification Behavior in a Bubbling Fluidized Bed Reactor: A Comparison between Biomass with and without Chemical Additives. *Energy Fuels* **2020**, *34*, 9654–9663. [CrossRef]
103. Kang, P.; Hu, X.E.; Lu, Y.; Wang, K.; Zhang, R.; Han, L.; Yuan, H.; Chen, H.; Luo, X.; Zhou, Y.J. Modeling and Optimization for Gas Distribution Patterns on Biomass Gasification Performance of a Bubbling Spout Fluidized Bed. *Energy Fuels* **2020**, *34*, 1750–1763. [CrossRef]
104. Lardier, G.; Kaknics, J.; Dufour, A.; Michel, R.; Cluet, B.; Authier, O.; Poirier, J.; Mauviel, G. Gas and Bed Axial Composition in a Bubbling Fluidized Bed Gasifier: Results with Miscanthus and Olivine. *Energy Fuels* **2016**, *30*, 8316–8326. [CrossRef]
105. Niu, M.; Huang, Y.; Jin, B.; Liang, S.; Dong, Q.; Gu, H.; Sun, R. A novel two-stage enriched air biomass gasification for producing low-tar high heating value fuel gas: Pilot verification and performance analysis. *Energy* **2019**, *173*, 511–522. [CrossRef]
106. Lin, C.-L.; Chou, J.-D.; Iu, C.-H. Effects of second-stage bed materials on hydrogen production in the syngas of a two-stage gasification process. *Renew. Energy* **2020**, *154*, 903–912. [CrossRef]
107. Zhu, H.L.; Zhang, Y.S.; Materazzi, M.; Aranda, G.; Brett, D.J.L.; Shearing, P.R.; Manos, G. Co-gasification of beech-wood and polyethylene in a fluidized-bed reactor. *Fuel Process. Technol.* **2019**, *190*, 29–37. [CrossRef]
108. Valdés, C.F.; Chejne, F.; Marrugo, G.; Macias, R.J.; Gómez, C.A.; Montoya, J.I.; Londoño, C.A.; De la Cruz, J.; Arenas, E. Co-gasification of sub-bituminous coal with palm kernel shell in fluidized bed coupled to a ceramic industry process. *Appl. Therm. Eng.* **2016**, *107*, 1201–1209. [CrossRef]
109. Couto, N.; Monteiro, E.; Silva, V.; Rouboa, A. Hydrogen-rich gas from gasification of Portuguese municipal solid wastes. *Int. J. Hydrogen Energy* **2016**, *41*, 10619–10630. [CrossRef]
110. Kaushal, P.; Tyagi, R. Advanced simulation of biomass gasification in a fluidized bed reactor using ASPEN PLUS. *Renew. Energy* **2017**, *101*, 629–636. [CrossRef]
111. Prestipino, M.; Chiodo, V.; Maisano, S.; Zafarana, G.; Urbani, F.; Galvagno, A. Hydrogen rich syngas production by air-steam gasification of citrus peel residues from citrus juice manufacturing: Experimental and simulation activities. *Int. J. Hydrogen Energy* **2017**, *42*, 26816–26827. [CrossRef]
112. Peng, W.X.; Wang, L.S.; Mirzaee, M.; Ahmadi, H.; Esfahani, M.J.; Fremaux, S. Hydrogen and syngas production by catalytic biomass gasification. *Energy Convers. Manag.* **2017**, *135*, 270–273. [CrossRef]
113. Liu, C.; Huang, Y.; Niu, M.; Pei, H.; Liu, L.; Wang, Y.; Dong, L.; Xu, L. Influences of equivalence ratio, oxygen concentration and fluidization velocity on the characteristics of oxygen-enriched gasification products from biomass in a pilot-scale fluidized bed. *Int. J. Hydrogen Energy* **2018**, *43*, 14214–14225. [CrossRef]
114. Savuto, E.; Di Carlo, A.; Steele, A.; Heidenreich, S.; Gallucci, K.; Rapagnà, S. Syngas conditioning by ceramic filter candles filled with catalyst pellets and placed inside the freeboard of a fluidized bed steam gasifier. *Fuel Process. Technol.* **2019**, *191*, 44–53. [CrossRef]
115. Jin, K.; Ji, D.; Xie, Q.; Nie, Y.; Yu, F.; Ji, J. Hydrogen production from steam gasification of tableted biomass in molten eutectic carbonates. *Int. J. Hydrogen Energy* **2019**, *44*, 22919–22925. [CrossRef]
116. Ismail, T.M.; Ramos, A.; Monteiro, E.; El-Salam, M.A.; Rouboa, A. Parametric studies in the gasification agent and fluidization velocity during oxygen-enriched gasification of biomass in a pilot-scale fluidized bed: Experimental and numerical assessment. *Renew. Energy* **2020**, *147*, 2429–2439. [CrossRef]
117. Mallick, D.; Mahanta, P.; Moholkar, V.S. Co-gasification of biomass blends: Performance evaluation in circulating fluidized bed gasifier. *Energy* **2020**, *192*, 116682. [CrossRef]
118. Inayat, A.; Khan, Z.; Aslam, M.; Shahbaz, M.; Ahmad, M.M.; Mutalib, M.I.A.; Yusup, S. Integrated adsorption steam gasification for enhanced hydrogen production from palm waste at bench scale plant. *Int. J. Hydrogen Energy* **2020**. [CrossRef]
119. Kibret, H.A.; Kuo, Y.-L.; Ke, T.-Y.; Tseng, Y.-H. Gasification of spent coffee grounds in a semi-fluidized bed reactor using steam and CO2 gasification medium. *J. Taiwan Inst. Chem. Eng.* **2021**, *119*, 115–127. [CrossRef]
120. Shahbaz, M.; Yusup, S.; Inayat, A.; Patrick, D.O.; Ammar, M.; Pratama, A. Cleaner Production of Hydrogen and Syngas from Catalytic Steam Palm Kernel Shell Gasification Using CaO Sorbent and Coal Bottom Ash as a Catalyst. *Energy Fuels* **2017**, *31*, 13824–13833. [CrossRef]
121. Tian, Y.; Zhou, X.; Lin, S.; Ji, X.; Bai, J.; Xu, M. Syngas production from air-steam gasification of biomass with natural catalysts. *Sci. Total Environ.* **2018**, *645*, 518–523. [CrossRef] [PubMed]
122. Kumar, A.; Guangul, F.M.; Inayat, M.; Sulaiman, S. Effect of fuel particle size and blending ratio on syngas production and performance of co-gasification. *J. Mech. Eng. Sci.* **2016**, *10*, 2188.

123. Madadian, E.; Orsat, V.; Lefsrud, M. Comparative Study of Temperature Impact on Air Gasification of Various Types of Biomass in a Research-Scale Down-draft Reactor. *Energy Fuels* **2017**, *31*, 4045–4053. [CrossRef]
124. Abdoulmoumine, N.; Kulkarni, A.; Adhikari, S. Effects of temperature and equivalence ratio on mass balance and energy analysis in loblolly pine oxygen gasification. *Energy Sci. Eng.* **2016**, *4*, 256–268. [CrossRef]